Methodology for pH measurement in high alkali cementitious systems

Brian Traynor [a], Hugo Uvegi [a], Elsa Olivetti [a], Barbara Lothenbach [b], Rupert J. Myers [c,d,*]

[a] Department of Materials Science and Engineering, Massachusetts Institute of Technology, 77 Massachusetts Avenue, Cambridge, Massachusetts, 01239, United States

[b] EMPA, Laboratory for Concrete & Construction Chemistry, CH-8600 Dübendorf, Switzerland

[c] School of Engineering, University of Edinburgh, Edinburgh, EH9 3FB, UK

[d] Current address: Department of Civil and Environmental Engineering, Imperial College London, Skempton Building, London, SW7 2AZ, UK

* Corresponding author. Email: r.myers@imperial.ac.uk

Keywords: pH, alkalis, pore solution

Abstract

A methodology for calibrating pH meters in highly alkaline solutions such as those relevant to cementitious systems is presented. This methodology uses an extended form of the Debye-Hückel equation to generate a calibration curve of pH vs. the measured electrochemical potential (mV) based on a series of aqueous alkali hydroxide solutions of known concentrations. This methodology is compared with the 'built-in' process of calibration based upon pH 4, 7, and 10 standard solutions. The built-in calibration process underestimates the real pH values by up to 0.3 log units, which is attributed to the alkali error. A spreadsheet for determining the calibration curve and its application to pH meter readings is provided as

Supporting Information. The implications of improperly calibrated pH meters on interpreting solution chemistry in cementitious systems are discussed.

1. Introduction

Measurement of pH is a quick, simple and cost-effective technique that is fundamental to analytical chemistry and widely used in cement science. Fresh Portland cement concrete typically has a pH > 13 [1]. Maintaining such a high pH is essential to ensure passivation of steel in reinforced concrete, thereby preventing structural deterioration [2,3]. The pH of the activator solution in an alkali-activated material plays a critical role in precursor dissolution [4,5], and high pH solutions (> 13) are typically employed for this purpose [6]. In both Portland cement and alkali-activated material systems, the formation of reaction products has also been shown to depend on pH [7–10].

Calibration of a pH meter is necessary for accurate pH measurements. pH meters are typically calibrated using standard solutions with pH values of 4, 7, and 10 – a process we refer to here as the 'built-in' pH meter calibration. Saturated aqueous $Ca(OH)_2$ solution may be used as a pH 12.45 standard (at 25°C) [11]. However, these pH values are below the pH range of most cementitious systems; therefore, using the built-in calibration in cementitious systems will likely lead to systematic pH measurement errors. Through appropriate selection of solutions of known concentration, pH meters can be accurately calibrated to higher pH. Although versions of this methodology have been used for years in analyses of cementitious systems [1,12–17], it has been poorly explicitly disseminated and there has been relatively little uptake of it among the broader cement science community. This communication is intended to clarify this methodology to the cement science community at large. As such, a pH

calculator for NaOH and KOH solutions as a function of temperature and concentration is included in the Supporting Information and the relevant physical chemistry concepts underpinning these calculations are discussed here.

2. Background

Table 1. Nomenclature of terms

a_i	Activity of ion i
b_i	Molality (mol kg^{-1})
b_0	Standard molality, defined as 1 mol kg^{-1}
γ_i	Activity coefficient of ion i
z_i	Charge on ion i
I	Ionic strength, $= \frac{1}{2}\sum_i b_i z_i^2$ (mol kg^{-1})
$\dot{a}$	Distance of closest approach parameter of interacting ions in Debye-Hückel equation (Å)
b_γ	Semi-empirical parameter in extended Debye-Hückel equation (kg mol^{-1})
A_γ	Electrostatic parameter in Debye-Hückel equation (kg$^{1/2}$ mol$^{-1/2}$)
B_γ	Electrostatic parameter in Debye-Hückel equation (kg$^{1/2}$ mol$^{-1/2}$ Å^{-1})
x_{jw}	Amount of water, parameter in Debye-Hückel equation (mol)
X_w	Total amount of all species in the aqueous phase, parameter in Debye-Hückel equation (mol)
M_i	Molarity (mol L^{-1})

2.1. Activity of non-ideal solutions

We begin the description of our methodology to calibrate pH meters by expressing the acidity of a solution using pH values (Eq.(1)):

$$\mathrm{pH} = -\log_{10}(a_{H^+}) = -\log_{10}\left(\gamma_{H^+}\frac{b_{H^+}}{b_0}\right) \quad (1)$$

where a_{H^+} is the activity of aqueous H^+, b_{H^+} is the molality of aqueous H^+ (mol kg^{-1}, i.e., mol of aqueous H^+ per kg of solvent), b_0 is the standard molality which is defined as 1 mol kg^{-1} (included to make the activity dimensionless), and γ_{H^+} is the activity coefficient of aqueous H^+. Activity is a measure of the effective concentration of an ion in solution, accounting for non-idealities that arise in real solutions. Molality is the preferred thermodynamic expression for concentration due to its independence of temperature and pressure, unlike molarity (mol L^{-1}).

Deviations between activity and concentration arise from electrostatic interactions among ions in aqueous ionic solutions. Long range inter-ionic coulombic attractions affect ion activity predominantly at low concentrations, whereas short-range ion-ion and water-ion solvation interactions have additional effects at higher concentrations. Short-range ion-ion interactions (ion association) decrease ion activity through formation of ion-ion pairs, reducing the effective number of ions in solution. Water-ion solvation interactions (ion hydration) increase activity by effectively reducing the amount of solvent. In highly dilute aqueous environments, the difference between concentration and activity is negligible.

Debye-Hückel (DH) theory [18] was developed to calculate the mean activity coefficients of ions as a function of the concentration of ions in aqueous ionic solutions. DH theory as originally developed is applicable to dilute aqueous ionic solutions, in which short range

interactions are ignored by assuming a structureless solvent, and where the primary interactions between ions are long-range Coulombic forces. The theory results in the Debye-Hückel equation (Eq. (2)), which we define here using molalities:

$$\log_{10}\gamma_i = \frac{-A_\gamma z_i^2 \sqrt{I}}{1+\dot{a}B_\gamma\sqrt{I}} + \log_{10}\frac{x_{jw}}{X_w} \quad (2)$$

where z_i is the charge of ion *i* in solution, $\dot{a}$ (Å) is the average distance of closest approach of two ions of opposite charge, I (mol kg^{-1}) is the ionic strength (defined in Table 1), and A_γ (kg$^{1/2}$ mol$^{-1/2}$) and B_γ (kg$^{1/2}$ mol$^{-1/2}$ Å^{-1}) are parameters dependent on the temperature, density, and relative permittivity of the solvent (see Supporting Information). The average distance of closest approach, $\dot{a}$, does not in reality represent the sum of the ionic radii of the two ions, and in practice is adjusted to provide a best fit for the aqueous ionic solution of interest [19]. The second term in Eq. (2) contains the amount of water, x_{jw} (mol), and the total amount of species in the aqueous phase, X_w (mol) and changes the units of γ_i from molar fraction to molal fraction, aligning with our definition of activity. A more detailed derivation and explanation of this equation and related terms may be found in Wright [20]. The ionic strength is a measure of the molality of fully dissociated ions in solution, noting that only in very dilute solutions can salts be assumed to be completely dissociated. Eq. (2) is accurate in solutions up to moderate ionic strength, $I \leq 0.1$ mol kg^{-1} [21].

Versions of the Debye-Hückel equation with an extended term have been used by researchers to extend the range of ionic strengths over which Debye-Hückel theory is valid. Helgeson extended the DH equation with a linear term [19];

$$\log_{10}\gamma_i = \frac{-A_\gamma z_i^2\sqrt{I}}{1+\dot{a}B_\gamma\sqrt{I}} + b_\gamma I + \log_{10}\frac{x_{jw}}{X_w} \quad (3)$$

where b_γ (kg mol^{-1}) is a semi-empirical parameter, known as the extended term. In his model, a common distance of closest approach was assumed by Helgeson for all ions in a given aqueous ionic solution – values of $\dot{a}$ were calculated for various solutions, with $\dot{a}$ taking a common value for all ions in that solution. This assumption makes the Helgeson extension to the DH equation more accurate in solutions in which the primary salt concentration exceeds that of other aqueous ions. Additionally, the effects of short-range water-ion solvation interactions are captured by the extended term, b_γ (kg mol^{-1}). Helgeson described the solvation of an ion in solution using the Born equation [22], as corrected by Bjerrum [23], to calculate values of b_γ for various aqueous ionic solutions. The applicability of the Helgeson form of the Debye-Hückel (H-DH) equation at high ionic strengths depends on the aqueous ionic solution of interest. For aqueous NaOH and KOH solutions, the H-DH equation is accurate up to ionic strengths of 4.5 mol kg^{-1}, determined by Helgeson as the range of validity for the extended term, b_γ, through comparison of activity coefficients reported in the literature to those computed using the H-DH equation [19]. Two other notable forms of the extended DH equation are the Davies' equation and the Truesdell-Jones equation – these are discussed in the Supporting Information and are applicable at moderate to high ionic strengths, (I < 0.1 mol kg^{-1}, and I < 1 mol kg^{-1}, respectively) [26,27].

The Pitzer equations are suitable for high ionic strengths and mixed ion aqueous ionic solutions (I > 1 mol kg^{-1}) [28,29]; however, they require specific interaction parameters between aqueous species to be defined, which are numerous in cementitious systems (Ca^{2+}, $CaOH^+$, $SiO(OH)_3^-$, $SiO_2(OH)_2^{2-}$, etc.). Therefore, the Pitzer equations are less pragmatic for

application in cementitious systems than the extended forms of the DH equation and are not discussed further here.

2.2. pH measurement with a glass combination electrode

While activity cannot be directly measured, electrochemical potential can. pH is most commonly determined indirectly through measurement of an electrochemical potential using a pH meter, which typically consists of a glass combination electrode and a meter. The electrochemical potential of standard solutions with precisely known pH can be measured using a glass combination electrode, and a calibration curve of pH vs. electrochemical potential is generated by the meter. This built-in calibration curve is used to convert electrochemical potentials measured by the glass combination electrode in an analyte to pH. The electrochemical potential measured by the glass combination electrode, E_T, may be written as (Eq. (4)):

$$E_T = \varepsilon + E(a_{H^+}) \tag{4}$$

where ε (mV) is an electrochemical potential due to a combination of smaller potentials that are artifacts of the design of the glass combination electrode, (see Supporting Information), and $E(a_{H^+})$ (mV) is an electrochemical potential that is a function of solution pH. While Eq. (4) is similar to the Nernst equation ($E = E_0 - 2.303\frac{RT}{F}pH$), Eq. (4) is more appropriate in this context as the measured electrochemical potential, E_T, is not a linear function over the entire pH scale, as is implied by the Nernst equation. Despite this non-linearity, calibrations performed relating $E(a_{H^+})$ to pH are generally assumed to be linear. This is valid over most

158 of the pH range, but not for highly acidic or alkaline solutions, where linearity between
159 electrochemical potential and pH is lost.
160
161 The Ag/AgCl glass combination electrode with ion selective membrane is the most common
162 type of electrode used in pH meters. The potential of interest in this paper is the gel layer
163 potential, $E(a_{H^+})$, which occurs at the ion selective membrane of the glass combination
164 electrode. It arises due to the difference between H^+ activity in the external analyte electrolyte
165 and the inner buffer electrolyte. The glass membrane is a silicate glass with ion inclusions,
166 typically Ca^{2+}, Na^+, and Li^+, but the exact glass composition depends on the analyte ions
167 towards which the membrane is designed to be selective [30,31]. The gel layer potential,
168 which is generated across the glass membrane when in contact with the analyte, arises
169 through formation of a charged hydrated gel layer produced on either side of the glass
170 membrane [32,33].
171
172 Although the gel layer potential, $E(a_{H^+})$, is designed to change only as a function of analyte
173 H^+ ion activity (over a wide range of H^+ activities and analyte chemistries), no glass
174 membrane is ever wholly selective to one specific ion [34]. In highly alkaline solutions the
175 hydrated gel layer has a negative structural charge and is charge-balanced significantly by
176 aqueous alkali metal complexes (e.g., Na^+) in addition to H^+, as described by Baucke [35].
177 Cheng described the gel layer potential as a capacitor, in which the surface charge density,
178 caused by adsorbed ions (e.g., H^+, OH^-, Na^+), yields a potential across the glass membrane
179 [36]. In any case, the presence of positively charged alkali ions in the gel layer artificially
180 lowers the measured pH as alkali ions, rather than H^+ ions, contribute to the gel layer
181 potential. This phenomenon is known as the alkali error [37–39]. It arises when measuring
182 pH of highly alkaline aqueous solutions; the effect is relatively weak in the case of K^+,

183 moderate for Na^+, and strong for Li^+. Standard solutions of pH 4, 7, and 10 are thus
184 insufficient to calibrate a pH meter for measurement of highly alkaline aqueous solutions.
185 Calibrating a pH meter with solutions of similar chemistry and ionic strength to the analyte is
186 a means of providing a valid calibration curve by mitigating the systematic errors discussed
187 above, including the alkali error [40].
188
189 In the context of cement science, the observed discrepancies between measured and actual pH
190 can significantly alter interpretation of experimental results. As discussed in the introduction,
191 the evolution of a (solid/liquid) cementitious system depends on the OH^- concentration in its
192 aqueous phase. Dissolution rates of a wide range of minerals and cement hydration products
193 have shown strong dependences on pH, with small differences in pH potentially
194 corresponding to large changes in rates of dissolution [41–46]. Similarly, the rates and
195 distributions of reaction products vary with pH [4,7]. For example, pH affects silicate
196 speciation in aqueous alkali silicate solutions [47], and the relative stabilities of calcium
197 (alkali) (alumino)silicate hydrate (C-(N-)A-S-H) and portlandite [48], and zeolites and alkali
198 aluminosilicate (hydrate) gel [7,49–51]. We draw attention to the fact that misinterpretation
199 of pore solution chemistry of a cementitious system can lead to mis-characterization of its
200 solid phases due to the intrinsic link between solid and liquid phases (e.g., equilibrium
201 phenomena), which is relevant to systems involving pure solid phases, binders, mortar, and
202 concrete. Aqueous solutions of NaOH and KOH are of interest in cementitious systems due
203 to their use in AAMs and the relatively high concentrations of these alkali metals (K
204 especially) in hydrated Portland cement.
205
206 The H-DH equation allows calculation of the activity of OH^-, and hence pH, up to ionic
207 strengths of 4.5 mol kg^{-1} for single component aqueous systems [19] or 1-3 mol kg^{-1} in

multi-component cementitious systems [48]. For solutions of known molarity, a calibration curve can be constructed through the electrochemical response of the pH meter in solution and the pH determined using the H-DH equation for each solution. By accounting for the alkali error in this way, the pH of an analyte can be accurately determined. We demonstrate the use of this methodology in the following sections of this paper.

3. Experimental procedures

3.1. NaOH and KOH standards, and LiOH solutions

NaOH and KOH standards were prepared with the following concentrations: 0.0001 M (mol L^{-1}), 0.0005 M, 0.001 M, 0.005 M, 0.01 M, 0.05 M, 0.1 M, 0.2 M, 0.5 M, 1 M, 2 M, and 3 M. NaOH and KOH standards were made by diluting commercial solutions of 3 (±0.005) M NaOH (BDH Chemicals) and 8 (±0.005) M KOH (Ricca), respectively. Dilutions were performed by transferring quantities of Na(K)OH commercial solution into volumetric flasks and filling to their marks with high purity water (18.2 MΩ cm, Millipore). The as-ordered Na(K)OH commercial solutions were stored in high-density polyethylene (HDPE) bottles. All prepared solutions were stored in clean HDPE bottles upon preparation.

LiOH solutions (concentrations of 0.0001 M (mol L^{-1}), 0.0005 M, 0.001 M, 0.005 M, 0.01 M, 0.05 M, 0.1 M, 0.2 M, 0.5 M, 1 M, 2 M, and 3 M) were prepared by addition of appropriate quantities of reagent grade lithium hydroxide monohydrate flakes (> 98%, Alfa Aesar) to a 500 mL volumetric flask and filling to the mark with high purity water (18.2 MΩ cm, Millipore) once flakes had completely dissolved. Calibrations used freshly prepared solutions to mitigate effects of carbonation of alkalis. The use of analytical grade salts in the

case of LiOH can lead to higher deviations (±2%) from the target concentrations than the use of standard solutions in the cases of KOH and NaOH. This has been taken into account in the calculated uncertainties of pH values reported here, resulting in a deviation of <0.001 pH units for the LiOH solutions.

3.2. pH measurements

A typical pH meter offers the possibility to read out i) the pH values directly based on the built-in calibration using pH 4, 7, and 10 standard solutions ('built-in calibration') or ii) the mV electrochemical potential (mV). All pH measurements were performed with a Thermo Orion Ag/AgCl combination triode stored in KCl solution with Automatic Thermal Correction probe at 22°C. Between measurement of each analyte, the pH meter was rinsed using water purified by reverse osmosis (18 MΩ cm) (Millipore) and gently dabbed dry using delicate wipes (Kimtech). Approximately 10 mL of prepared aqueous Na(K)OH solution was transferred to a 15 mL polypropylene (PP) centrifuge tube. The solution was gently agitated for a few seconds, and the electrochemical potential was recorded after 2 minutes (when the reading had stabilized). Samples were not stirred during pH measurements [52]. The main sources of error in this study were the accuracy of the pH meter and glass combination electrode in measuring the electrochemical potential (±0.2 mV), and the error in the built-in calibration slope recorded (±0.5 %). Errors in the calculated pH values are based on the standard deviation of recorded temperatures (±0.5 °C) during measurement of the pH of solutions. Error propagation calculations are included in the Supporting Information.

3.3. Fitted calibration curve calculations

The pH of the solution was calculated from the solution concentrations using the H-DH equation for aqueous NaOH and KOH solutions and known equilibrium constants for Na(K)OH dissociation at the measurement (laboratory) temperature (22°C) from [53]. The calculated pH values were then plotted against the measured electrochemical potentials of prepared Na(K)OH solutions using the pH meter, and the data fitted using a calibration curve ('fitted calibration'). The use of NaOH or KOH solutions for the fitted calibration directly takes into account the alkali error, as the same alkali error occurs both during the calibration and the measurement accounting for the systematic error. Electrochemical potentials of analytes are also measured using electrochemical potential (mV) readings from the pH meter, and the fitted calibration curve is used to convert the readings to pH. We provide a spreadsheet for the determination of this calibration curve and application to pH meter readings of sample solutions as Supporting Information.

3.4. Preparation of alkali-activated biomass ash samples

Application of this methodology to a real cementitious system is also demonstrated here. Alkali-activated biomass ash experiments were prepared using 0.5 and 1 molal aqueous NaOH solutions (ACS Reagent grade water, RICCA Chemical Company; NaOH ≥97%, Sigma Aldrich) as activators at a constant liquid/solid ratio of 25 (i.e. 2 g of solid in 50 mL of solution). Solids consisted of highly siliceous biomass ash (sourced from Silverton Pulp & Papers Pvt. Ltd. In Muzzafarnagar, Uttar Pradesh, India) and $Ca(OH)_2$ (≥98%, Macron Fine Chemicals), mixed at a ratio of 1.75 g ash : 0.25 g $Ca(OH)_2$. The composition of the biomass ash, determined by X-ray fluorescence and loss on ignition tests, showed siliceous ash (61 mass% SiO_2) with high unburnt carbon (26 mass%). The phase composition (determined by X-ray diffraction) showed a primarily amorphous ash (90 mass%) with presence of quartz,

albite, cristobalite, sylvite and arcanite. The materials and conditions of reaction were chosen to mimic a masonry product previously developed in [54]. Samples were mixed continuously in a tube rotator (Fisherbrand™ Multi-Purpose Tube Rotator, Fisher Scientific) to ages of 3 and 28 days to explore dissolution and reaction kinetics.

4. pH meter calibration

The linear calibration curve fittings for prepared aqueous NaOH and KOH solutions are respectively shown in Figure 1 (A) and (B). The alkali error associated with measuring the pH of LiOH solutions is also demonstrated (Figure 1 (C)). The pH is calculated using the H-DH equation (Eq. (3)) and methodology presented here and in the Supporting Information. The measured built-in pH is based on an extrapolated calibration curve using pH 4, 7, and 10 standard solutions. The divergence at high pH (Figure 1A, inset) demonstrates the alkali error and the need to apply the methodology presented here when measuring highly alkaline solutions, i.e., in analysis of cementitious systems.

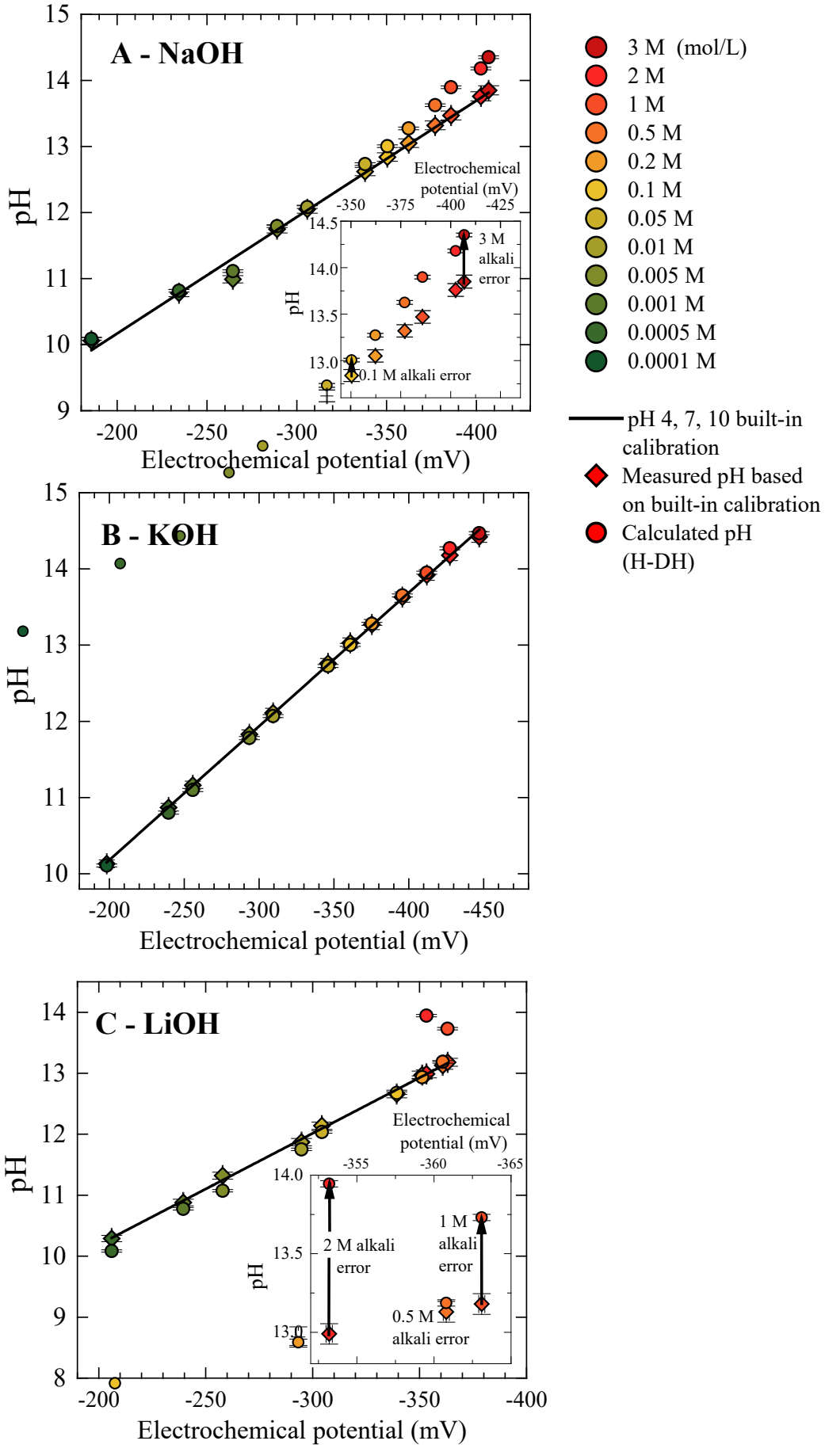
A - NaOH
pH
Electrochemical potential (mV)
Electrochemical potential (mV)
3 M alkali error
0.1 M alkali error
B - KOH
pH
Electrochemical potential (mV)
C - LiOH
pH
Electrochemical potential (mV)
2 M alkali error
1 M alkali error
0.5 M alkali error
3 M (mol/L)
2 M
1 M
0.5 M
0.2 M
0.1 M
0.05 M
0.01 M
0.005 M
0.001 M
0.0005 M
0.0001 M
pH 4, 7, 10 built-in calibration
Measured pH based on built-in calibration
Calculated pH (H-DH)

299

Figure 1. Calibration curves for aqueous NaOH (A), KOH (B), and LiOH (C) solutions of known concentration up to 3 M based upon pH values calculated using the H-DH equation (circles) and those measured by the pH meter using standard solutions of pH 4, 7, and 10 (triangles) at 22 °C. The deviation between the calculated pH and the uncorrected, extrapolated built-in calibration curve from pH 4, 7, 10 standards (black line) is a result of the alkali error at high pH, which is more pronounced for Li^+ and Na^+ than K^+. The solution molarities at which the alkali error is significant are shown in the inset graphs. For LiOH solutions, the pH was calculated using the Davies' equation, as the H-DH equation is not valid for LiOH solutions.

While the calculated pH (H-DH) does trend above the measured pH, the alkali error for pH measurement in aqueous KOH solutions is not statistically significant. In contrast, the alkali error for NaOH is up to 0.5 pH units in 3 M NaOH. The alkali error for LiOH solutions is even greater – the alkali error for 2 M LiOH solutions is 1 pH unit. The extent of the alkali error in LiOH solutions precludes any meaningful direct pH measurements above concentrations of 0.5 M LiOH [55]. This trend is explained in terms of ion size: K^+ ions (internuclear radius in aqueous solution of 2.8 Å [56]) are significantly less mobile through the glass membrane than Na^+ ions (internuclear radius in aqueous solution of 2.3 Å [56]) and Li^+ ions (internuclear radius in aqueous solution of 2.1 Å [56]), due to their smaller ion size [38,57].

The H-DH equation used above is designed for aqueous NaOH and KOH solutions [19] up to ionic strengths of 4.5 mol kg^{-1} [19], but in multi-component cementitious systems this range is typically taken as 1-3 mol kg^{-1} [48]. Parameters for the H-DH equation have also been calculated for other aqueous ionic solutions (HCl, LiCl, $MgCl_2$, $SrCl_2$, $CaCl_2$, $BaCl_2$, $AlCl_3$, HBr, LiBr, NaBr, $MgBr_2$, $SrBr_2$, $CaBr_2$, $BaBr_2$, HI, NaI, MgI_2, SrI_2, CaI_2, BaI_2, KF) [19]. The temperature at which the pH is recorded is important for H-DH calculations – the dissociation constants of NaOH, KOH, and H_2O change with temperature (see Supporting Information) [58], affecting the OH^- concentration.

5. Application to cementitious systems

To demonstrate the utility of the methodology presented, pH values of filtrates taken from a series of alkali-activated biomass ash samples were measured. In each case, we use the NaOH fitted calibration curve (Figure 1A) to convert the measured electrochemical potential to pH. Details on how these samples were made are given in the Section 3.4. The results of the pH measurements and calculations using the methodology presented here are shown in Table 2.

Table 2. OH^- concentrations and pH of samples measured using calibration curve (calculated from H-DH equation, Figure 1A, circles) at 22 °C.

Initial b_{NaOH} (mol kg^{-1})	Biomass Ash Mass (g)	$Ca(OH)_2$ Mass (g)	Curing time (days)	Electro-chemical potential (mV)	Built-in[1] pH (-)	$b_{[OH-]}$[2] (mol kg^{-1})	Fitted[2] pH (-)
0.5	0	0	3	-372.4	13.33±0.07	0.406	13.62±0.02
			28	-371.3	13.31±0.07	0.385	13.60±0.02
	2	0	3	-361.9	13.15±0.07	0.244	13.41±0.02
			28	-352.4	12.97±0.06	0.153	13.22±0.02
	1.75	0.25	3	-365.2	13.21±0.07	0.287	13.48±0.02
			28	-356.4	13.04±0.07	0.186	13.30±0.02
1	0	0	3	-381.4	13.49±0.07	0.617	13.80±0.02
			28	-380.1	13.46±0.07	0.582	13.77±0.02
	2	0	3	-372.6	13.32±0.07	0.410	13.62±0.02
			28	-369.4	13.26±0.07	0.352	13.56±0.02
	1.75	0.25	3	-374.9	13.37±0.07	0.457	13.67±0.02
			28	-372.3	13.31±0.07	0.404	13.62±0.02

[1] Obtained directly from the built-in pH meter calibration using pH 4, 7, and 10 standard solutions. The differences from the calculated pH values are due to the alkali error

[2] OH^- concentration and fitted pH calculated from fitted calibration curve derived using the H-DH equation

Differences between the calculated and measured pH, i.e., the alkali error, are consistently on the order of 0.3 pH units, corresponding to an underestimation of b_{OH-} by 0.25 mol kg^{-1} if the built-in calibration is used. Samples with higher pH values differ more greatly from the actual pH, as expected. For context, at 22 °C the calculated (H-DH) pH values of 1 and 0.5 mol kg^{-1} aqueous NaOH solutions are 13.86 and 13.59, respectively. The difference of 0.27 pH units is

similar to the discrepancy caused by the alkali error (0.3 pH units), demonstrating the effect of this phenomenon in analysis of cementitious systems.

6. Conclusions

A methodology for calibrating pH meters in solutions of high alkali content (pH >13) has been presented. The Helgeson extension to the Debye-Hückel (H-DH) equation was used to calculate the pH of aqueous ionic solutions of known molarity. The H-DH equation was chosen because of its practicality and accuracy at high ionic strengths (approaching 4.5 mol kg^{-1}). We provide a spreadsheet for the determination of this calibration curve and application to pH meter readings of sample solutions as Supporting Information. The value of this methodology was demonstrated for a binder consisting of biomass ash, $Ca(OH)_2$ and aqueous NaOH activator. The discrepancies, caused by the alkali error, between the actual, fitted pH (calculated using the H-DH) and the measured pH (based on the built-in pH 4, 7, 10 standards calibration) were highlighted. The built-in calibration underestimated the real pH values by up to 0.3 pH units in aqueous NaOH solution, which illustrates the importance of a properly calibrated pH meter to prevent erroneous interpretations of the pH of cementitious systems. Discrepancies between built-in calibration and real, fitted pH values were more pronounced for aqueous LiOH solutions compared to aqueous NaOH solutions, but less so for aqueous KOH solutions.

7. Supporting information

Two files are provided as supporting information: (1) a document containing additional descriptions of (S1) other forms of the extended Debye-Hückel equation, (S2)

electrochemical potentials in glass combination electrodes, and (S3) the error analysis performed here; and (2) a spreadsheet embedded with calculations and a step-by-step procedure to use the method described here, to measure pH in high alkali cementitious systems.

8. Acknowledgments

We would like to acknowledge the financial support for this research through the Environmental Solutions Initiative at Massachusetts Institute of Technology (MIT), Cambridge. We also acknowledge support from NSF CAREER #1751925. Funding provided by the Scottish Research Partnership in Engineering Grant #PECRE1718/02 is gratefully acknowledged. The research leading to this publication benefitted from EPSRC funding under grant No. EP/R010161/1 and from support from the UKCRIC Coordination Node, EPSRC grant number EP/R017727/1, which funds UKCRIC's ongoing coordination.

9. Conflicts of interest

The authors declare no conflicts of interest.

10. References

[1] B. Lothenbach, F. Winnefeld, Thermodynamic modelling of the hydration of Portland cement, Cem. Concr. Res. 36 (2006) 209–226. doi:10.1016/j.cemconres.2005.03.001.

[2] A.M. Vaysburd, P.H. Emmons, Corrosion inhibitors and other protective systems in concrete repair: Concepts or misconcepts, Cem. Concr. Compos. 26 (2004) 255–263.

doi:10.1016/S0958-9465(03)00044-1.

[3] C.L. Page, K.W.J. Treadaway, Aspects of the electrochemistry of steel in concrete, Nature. 297 (1982) 109–115.

[4] S. Song, H.M. Jennings, Pore solution chemistry of alkali-activated ground granulated blast-furnace slag, Cem. Concr. Res. 29 (1999) 159–170. doi:10.1016/S0008-8846(98)00212-9.

[5] S. Goto, K. Akawaza, M. Daimon, Solubility of silica-alumina gels in different pH solutions, Cem. Concr. Res. 22 (1992) 1216–1223.

[6] J.L. Provis, S.A. Bernal, RILEM State of the Art Report, 2014. doi:10.1007/978-94-007-7672-2_5.

[7] C.K. Yip, G.C. Lukey, J.S.J. Van Deventer, The coexistence of geopolymeric gel and calcium silicate hydrate at the early stage of alkaline activation, Cem. Concr. Res. 35 (2005) 1688–1697. doi:10.1016/j.cemconres.2004.10.042.

[8] J.G.S. Van Jaarsveld, J.S.J. Van Deventer, Effect of the alkali metal activator on the properties of fly ash-based geopolymers, Ind. Eng. Chem. Res. 38 (1999) 3932–3941. doi:10.1021/ie980804b.

[9] B. Mota, T. Matschei, K. Scrivener, Impact of NaOH and Na2SO4 on the kinetics and microstructural development of white cement hydration, Cem. Concr. Res. 108 (2018) 172–185. doi:10.1016/j.cemconres.2018.03.017.

[10] E. L'Hôpital, B. Lothenbach, K. Scrivener, D.A. Kulik, Alkali uptake in calcium alumina silicate hydrate (C-A-S-H), Cem. Concr. Res. 85 (2016) 122–136. doi:10.1016/j.cemconres.2016.03.009.

[11] R.G. Bates, V.E. Bower, E.R. Smith, Calcium hydroxide as a highly alkaline pH standard, J. Res. Natl. Bur. Stand. (1934). 56 (1956) 305–312. doi:10.6028/jres.056.040.

[12] R.J. Myers, E. L'Hôpital, J.L. Provis, B. Lothenbach, Effect of temperature and aluminium on calcium (alumino)silicate hydrate chemistry under equilibrium conditions, Cem. Concr. Res. 68 (2015) 83–93. doi:10.1016/j.cemconres.2014.10.015.

[13] D.E. MacPhee, K. Luke, F.P. Glasser, E.E. Lachowski, Solubility and aging of calcium silicate hydrates in alkaline solutions at 25°C, J. Am. Ceram. Soc. 72 (1989) 646–654.

[14] D. Rothstein, J.J. Thomas, B.J. Christensen, H.M. Jennings, Solubility behavior of Ca-, S-, Al-, and Si-bearing solid phases in Portland cement pore solutions as a function of hydration time, Cem. Concr. Res. 32 (2002) 1663–1671.

[15] A. Kumar, S. Bishnoi, K.L. Scrivener, Modelling early age hydration kinetics of alite, Cem. Concr. Res. 42 (2012) 903–918. doi:10.1016/j.cemconres.2012.03.003.

[16] Gartner, F.J. Tang, S.J. Weiss, Saturation factors for calcium hydroxide and calcium sulfates in fresh Portland cement pastes, J. Am. Ceram. Soc. 68 (1985) 667–673. doi:10.1111/j.1151-2916.1985.tb10122.x.

[17] G. Plusquellec, M.R. Geiker, J. Lindgård, J. Duchesne, B. Fournier, K. De Weerdt, Determination of the pH and the free alkali metal content in the pore solution of concrete: Review and experimental comparison, Cem. Concr. Res. 96 (2017) 13–26. doi:10.1016/j.cemconres.2017.03.002.

[18] P. Debye, E. Huckel, Zur Theorie der Elektrolyte, Z. Phys. 24 (1923) 185–206.

[19] H.C. Helgeson, D.H. Kirkham, G.C. Flowers, Theoretical prediction of the thermodynamic behavior of-aqueous electrolytes at high pressures and temperatures: IV. Calculation of activity coefficients, osmotic coefficients, and apparent molal and standard and relative partial molal properties to 600C, Am. J. Sci. 281 (1981) 1249–1516.

[20] M. Robson Wright, Chapter 10: Concepts and Theory of Non-Ideality, in: An Introd. to Aqueous Electrolyte Solut., Wiley, 2007: pp. 349–420.

[21] J.F. Zemaitis, D.M. Clark, M. Rafal, N.C. Scrivner, Handbook of Aqueous Electrolyte Thermodynamics, 1986.

[22] M. Born, Volumen und hydratationswärme der ionen, Zeitschrift Für Phys. 1 (1920) 45–48.

[23] N. Bjerrum, Neuere Anschauungen über Elektrolyte, Berichte Der Dtsch. Chem. Gesellschaft. 62 (1929) 1091–1103.

[24] I. Grenthe, A. V. Plyasunov, K. Spahiu, Chapter IX: Estimations of Medium Effects on Thermodynamic Data, 1997.

[25] M. Wang, Y. Zhang, M. Muhammed, Critical evaluation of thermodynamics of complex formation of metal ions in aqueous solutions I. A description of evaluation methods, Hydrometallurgy. 45 (1997) 21–36.

[26] C.W. Davies, Ion Association, Butterworth and Co, 1962.

[27] A.H. Truesdell, B.F. Jones, WATEQ: A computer program for calculating chemical equilibria of natural waters, Jour. Res. US Geol. Surv. 2 (1974) 233–248.

[28] K.S. Pitzer, Thermodynamics of electrolytes. I. Theoretical basis and general equations, J. Phys. Chem. 77 (1973) 268–277. doi:10.1021/j100621a026.

[29] R.P. Buck, S. Rondini, A.K. Covington, F.G.K. Baucke, C.M.A. Brett, M.J.T. Milton, T. Mussini, R. Naumann, K.W. Pratt, P. Spitzer, G.S. Wilson, Measurement of pH: Definition, Standards, and Procedures (IUPAC Recommendations 2002), Pure Appl. Chem. 74 (2002) 2169–2200.

[30] A.K. Covington, Chapter 5: Glass Electrodes, in: Ion Sel. Electrode Methodol. Vol 1, CRC Press, 1979: pp. 77–84.

[31] G. Eisenman, Chapter 3: The dependence of glass-electrode on composition, in: Glas. Electrodes Hydrog. Other Cations, New York, 1967: pp. 51–100.

[32] M. Cremer, Uber die ursache der elektromotorischen eigenschaften der gewebe

475 zugleich ein beitrag zur lehre von den polyphasischen elektrolytketten, Z Biol. 47
476 (1906) 562–608.
477 [33] D.A. Skoog, D.M. West, Fundamentals of Analytical Chemistry, 3rd ed., 1976.
478 [34] B.P. Nicolsky, M.M. Shultz, A.A. Belijustin, A.A. Lev, Chapter 6: Ion exchange
479 theory of the glass electrodes, in: G. Eisenman (Ed.), Glas. Electrodes Hydrog. Other
480 Cations, 1967: pp. 174–222.
481 [35] F.G.K. Baucke, The modern understanding of the glass electrode response, Fresenius.
482 J. Anal. Chem. 349 (1994) 582–596. doi:10.1007/BF00323462.
483 [36] K.L. Cheng, Capacitor theory for nonfaradaic potentiometry, Microchem. J. 42 (1990)
484 5–24.
485 [37] R.G. Bates, Determination of pH, in: 2nd ed., Wiley, New York, 1973: p. 365.
486 [38] K. Oláh, On the theory of the alkaline error of the glass electrode, Period. Polytech.
487 Chem. Eng. 4 (1960) 141–156.
488 [39] B.P. Nicolsky, Theory of the glass electrode. I., Zh Fis Khim. 10 (1937) 495.
489 [40] A.D. Wiesner, L.E. Katz, C. Chen, The impact of ionic strength and background
490 electrolyte on pH measurements in metal ion adsorption experiments, J. Colloid
491 Interface Sci. 301 (2006) 329–332. doi:10.1016/j.jcis.2006.05.011.
492 [41] J. Schott, O.S. Pokrovsky, E.H. Oelkers, The link between mineral
493 dissolution/precipitation kinetics and solution chemistry, Rev. Mineral. Geochemistry.
494 70 (2009) 207–258. doi:10.2138/rmg.2009.70.6.
495 [42] P. V. Brady, J. V. Walther, Controls on silicate dissolution rates in neutral and basic
496 pH solutions at 25°C, Geochim. Cosmochim. Acta. 53 (1989) 2823–2830.
497 doi:10.1016/0016-7037(89)90160-9.
498 [43] E.H. Oelkers, J. Schott, J.L. Devidal, The effect of aluminum, pH, and chemical
499 affinity on the rates of aluminosilicate dissolution reactions, Geochim. Cosmochim.

Acta. 58 (1994) 2011–2024. doi:10.1016/0016-7037(94)90281-X.

[44] I. Baur, P. Keller, D. Mavrocordatos, B. Wehrli, C.A. Johnson, Dissolution-precipitation behaviour of ettringite, monosulfate, and calcium silicate hydrate, Cem. Concr. Res. 34 (2004) 341–348. doi:10.1016/j.cemconres.2003.08.016.

[45] A. Gabrisová, J. Havlica, S. Sahu, Stability of calcium sulphoaluminate hydrates in water solutions with various pH values, Cem. Concr. Res. 21 (1991) 1023–1027. doi:10.1016/0008-8846(91)90062-M.

[46] P. Juilland, E. Gallucci, R. Flatt, K. Scrivener, Dissolution theory applied to the induction period in alite hydration, Cem. Concr. Res. 40 (2010) 831–844. doi:10.1016/j.cemconres.2010.01.012.

[47] J.L. Provis, P. Duxson, G.C. Lukey, F. Separovic, W.M. Kriven, J.S.J. Van Deventer, Modeling speciation in highly concentrated alkaline silicate solutions, Ind. Eng. Chem. Res. 44 (2005) 8899–8908. doi:10.1021/ie050700i.

[48] R.J. Myers, S.A. Bernal, J.L. Provis, A thermodynamic model for C-(N-)A-S-H gel: CNASH-ss. Derivation and validation, Cem. Concr. Res. 66 (2014) 27–47. doi:10.1016/j.cemconres.2014.07.005.

[49] H. Matsuyama, J.F. Young, Effects of pH on precipitation of quasi-crystalline calcium silicate hydrate in aqueous solution, Adv. Cem. Res. 12 (2000) 29–33. doi:10.1680/adcr.2000.12.1.29.

[50] I. García Lodeiro, D.E. Macphee, A. Palomo, A. Fernández-Jiménez, Effect of alkalis on fresh C–S–H gels. FTIR analysis, Cem. Concr. Res. 39 (2009) 147–153. doi:10.1016/j.cemconres.2009.01.003.

[51] B. Lothenbach, E. Bernard, U. Mäder, Zeolite formation in the presence of cement hydrates and albite, Phys. Chem. Earth. 99 (2017) 77–94. doi:10.1016/j.pce.2017.02.006.

525 [52] K.L. Cheng, D.M. Zhu, On calibration of pH meters, Sensors. 5 (2005) 209–219.
526 doi:10.3390/s5040209.
527 [53] T. Thoenen, W. Hummel, U.R. Berner, E. Curti, The PSI/Nagra Chemical
528 Thermodynamic Database 12/07, Villigen PSI, Switzerland, 2014.
529 [54] T. Poinot, M.E. Laracy, C. Aponte, H.M. Jennings, J.A. Ochsendorf, E.A. Olivetti,
530 Beneficial use of boiler ash in alkali-activated bricks, Resour. Conserv. Recycl. 128
531 (2018) 1–10. doi:10.1016/j.resconrec.2017.09.013.
532 [55] S. Licht, pH measurement in concentrated alkaline solutions, Anal. Chem. 57 (1985)
533 514–519. doi:10.1021/ac50001a045.
534 [56] Y. Marcus, Ionic radii in aqueous solutions, J. Solution Chem. 12 (1983) 271–275.
535 doi:10.1007/BF00646201.
536 [57] M. Dole, B.Z. Wiener, The theory of the glass electrode. IV. Temperature studies of
537 the glass electrode error, Trans. Electrochem. Soc. 72 (1937) 107–127.
538 [58] G.M. Anderson, D.A. Crerar, Thermodynamics in Geochemistry, Oxford University
539 Press, 1993.
540